Available online at www.sciencedirect.com
SCIENCE DIRECT®
ELSEVIER
Journal of Molecular Structure 705 (2004) 21–27
Journal of MOLECULAR STRUCTURE
www.elsevier.com/locate/molstruc

Solvothermal synthesis and structures of lanthanide-organic sandwich coordination polymers with 4,4′-biphenyldicarboxylic acid

Yi-Bo Wang[a], Wen-Juan Zhuang[a], Lin-Pei Jin[a,*], Shao-Zhe Lu[b]

[a]Department of Chemistry, Beijing Normal University, Beijing 100875, China
[b]Laboratory of Excited Process of Physics, Chinese Academy of Sciences, Changchun 130021, China

Received 16 January 2004; revised 13 April 2004; accepted 14 April 2004
Available online 17 July 2004

Abstract

First examples of lanthanide coordination polymers with 4,4′-biphenyldicarboxylic acid (4,4′-H_2bpdc), Ln(4,4′-Hbpdc)(4,4′-bpdc)$(H_2O)_2$ (Ln = Pr(1), Eu(**2**), Gd(**3**)) and Er(4,4′-bpdc)$_{1.5}$$(H_2O)_2$ (**4**) were prepared by the solvothermal synthesis. Crystallographic data show that complexes **1**–**3** are isostructural and each lanthanide(III) ion is coordinated to six 4,4′-Hbpdc ligands, and display 3D sandwich structure with lanthanide ion layers and organic ligand layers alternately linking up with each other. Complex **4** shows different coordination modes of 4,4′-bpdc ligands from **1**–**3** and each Er(III) ion is attached to four 4,4′-bpdc ligands to construct 3D sandwich structure. The emission spectrum of **2** shows one Eu^{3+} ion site, which is consistent with the results of the X-ray crystal structure analysis.

Keywords: Coordination polymers; Solvothermal synthesis; Lanthanide; X-ray diffraction; Coordination mode

1. Introduction

Coordination polymers are currently attracting considerable attention as a result of their distinctive properties and potential applications [1–4]. At the same time, in the course of the preparation of coordination polymers, design strategies for the prediction of coordination polymers are based on the theory in which solid-state architecture determines function through a controlled assembly of molecular components [5,6]. As is known to all, during the construction of 1D, 2D and 3D coordination polymers, the crystal architecture can be determined by the strength and directionality of covalent bonds and covalent metal–ligand bonds which are stronger than hydrogen bonds and other weak interactions, such as π–π stacking, etc. [7]. So metal–ligand interactions can be used in place of many weak interactions to direct the formation of metal–organic polymers.

4,4′-biphenyldicarboxylic acid (4,4′-H_2bpdc), acting as multi-coordination site ligand, has been received extensive attention and being well studied in transition metal coordination chemistry [4,8–13]. These transition metal coordination polymers containing 4,4′-bpdc ligands manifest 1D, 2D and 3D architecture, respectively, and usually display intriguing structure such as rectangular grids [12] and rhombic channels [4]. In the course of coordinating to metals, 4,4′-bpdc ligands will show various coordination modes. Consequently, their structural characteristics of two carboxyl groups lying at two opposite sites of the ligand may lead to interesting structure. Moreover, in view of lanthanide complexes with 2,2′-biphenyldicarboxylic acid (2,2′-bpdc) obtained in our previous work [14,15], the difference of carboxyl group positions between these two organic ligands maybe lead to completely different structures of lanthanide–bpdc complexes. Therefore, it is a good choice to employ 4,4′-bpdc ligand as a linear linker to build up lanthanide coordination polymers.

In this work, we introduce 4,4′-bpdc ligand into the construction of lanthanide coordination polymers to be up to each other for both diverse coordination modes of 4,4′-bpdc ligand and high coordination numbers of lanthanide ions, and finally obtain four new lanthanide–4,4′-bpdc ligand sandwich 3D coordination polymers with the formulae of Ln(4,4′-Hbpdc)(4,4′-bpdc)$(H_2O)_2$ (Ln = Pr(**1**), Eu(**2**),

* Corresponding author. Tel.: +86-106-220-5522; fax: +86-106-220-0567.
E-mail address: lpjin@bnu.edu.cn (L.-P. Jin).

0022-2860/$ - see front matter © 2004 Elsevier B.V. All rights reserved.
doi:10.1016/j.molstruc.2004.04.007

Gd(**3**)) and Er(4,4′-bpdc)$_{1.5}$(H_2O)$_2$ (**4**) by solvothermal reaction.

2. Experimental

$PrCl_3·7H_2O$, $EuCl_3·6H_2O$, $GdCl_3·6H_2O$, and $ErCl_3·6H_2O$ were prepared by dissolving their oxides in hydrochloric acid, respectively, and then dried. 4,4′-Biphenyldicarboxylic acid was purchased from Aldrich and used without further purification. While all the other reagents were commercially available and used as received.

2.1. Instrumentation

Elemental analyses were performed on an Elementar Vario EL analyzer. The IR spectra were recorded with a Nicolet Avatar 360 FT-IR spectrometer using the KBr pellet technique. Thermogravimetric analyses were performed on a ZRY-2P Thermal Analyzer.

The excitation light source was YAG-Nd laser that emits at 1.064 μm, and the excitation wavelength was 355 nm. The sample was placed in a Dewar and cooled with liquid nitrogen. The fluorescence was collected at right angles through a Spex 1403 monochromator with a photomultiplier tube, then averaged by Boxcar integrator and finally data were transferred to a computer.

The X-ray single crystal data collections for complexes **1**, **2**, **3** and **4** were performed on a Bruker Smart 1000 CCD diffractometer, using graphite-monochromated Mo Kα radiation ($\lambda = 0.71073$ Å). Semiempirical absorption corrections were applied using the SADABS program. The structures were solved by direct methods and refined by full-matrix least square on F^2 using the SHELXTL-97 program [16]. All non-hydrogen atoms were refined anisotropically. The hydrogen atoms were generated geometrically and treated by a mixture of independent and constrained refinement.

2.2. Syntheses of the four complexes

[Pr(4,4′-Hbpdc)(4,4′-bpdc)(H$_2$O)$_2$] (**1**) The mixture of $PrCl_3·7H_2O$ (0.072 g and 0.2 mmol), 4,4′-biphenyldicarboxylic acid (0.036 and 0.15 mmol), H_2O (5 ml), isopropyl alcohol (5 ml) and aqueous solution of NaOH (0.19 ml and 0.12 mmol) was sealed in a 25 ml stainless-steel reactor with Teflon liner and heated to 170 °C for 96 h, then slowly cooled to room temperature. Light green crystals of **1** were obtained in 24.3% (16 mg) yield. Anal. Calcd for $C_{28}H_{21}O_{10}Pr$: C, 51.04; H, 3.22. Found: C, 51.37; H, 2.93. IR data (KBr pellet, ν cm^{-1}): 676 (m), 701 (m), 744 (m), 770 (s), 1405 (s), 1527 (s), 1565 (m), 1585 (w), 1606 (m), 1633 (w), 3426 (s).

[Eu(4,4′-Hbpdc)(4,4′-bpdc)(H$_2$O)$_2$] (**2**) Synthesis of **2** was similar to **1**, and colorless crystals of **2** were obtained in 37.3% (25 mg) yield. Anal. Calcd for $C_{28}EuH_{21}O_{10}$: C, 50.19; H, 3.16. Found: C, 50.09; H, 2.86. IR data (KBr pellet, ν cm^{-1}): 675 (m), 701 (m), 744 (m), 769 (s), 1407 (s), 1531 (s), 1565 (m), 1586 (w), 1606 (m), 1647 (w), 3428 (s).

[Gd(4,4′-Hbpdc)(4,4′-bpdc)(H$_2$O)$_2$] (**3**) Synthesis of **3** was similar to **1**, and colorless crystals of **3** were obtained in 41.5% (28 mg) yield. Anal. Calcd for $C_{28}GdH_{21}O_{10}$: C, 49.80; H, 3.14. Found: C, 49.85; H, 2.79. IR data (KBr pallet, ν cm^{-1}): 675 (m), 700 (m), 745 (m), 769 (s), 1408 (s), 1533 (s), 1565 (m), 1586 (w), 1606 (m), 1652 (w), 3430 (s).

[Er(4,4′-bpdc)$_{1.5}$(H$_2$O)$_2$] (**4**) Synthesis of **4** was similar to **1** and light pink crystals of **4** were obtained in 26.6%

Table 1
Crystal data for **1**–**4**

Complexes	**1**	**2**	**3**	**4**
Empirical formula	$C_{28}H_{21}O_{10}Pr$	$C_{28}EuH_{21}O_{10}$	$C_{28}GdH_{21}O_{10}$	$C_{21}ErH_{16}O_8$
FW	658.36	669.41	674.70	563.60
Crystal system	Orthorhombic	Orthorhombic	Orthorhombic	Monoclinic
Space group	*Pbcn*	*Pbcn*	*Pbcn*	*P2(1)/c*
a (Å)	27.698(8)	27.565(10)	27.542(9)	15.990(6)
b (Å)	8.673(3)	8.619(3)	8.613(3)	7.578(3)
c (Å)	9.939(3)	9.905(4)	9.892(3)	17.294(6)
α (°)	90	90	90	90
β (°)	90	90	90	115.649(5)
γ (°)	90	90	90	90
Z	4	4	4	4
V (Å^3)	2387.7(13)	2353.1(14)	2346.7(13)	1889.0(12)
ρ_{calcd} (g cm$^{-3)}$	1.831	1.890	1.910	1.982
Temp (K)	293(2)	293(2)	293(2)	293(2)
μ (mm^{-1})	2.104	2.730	2.891	4.492
Reflections collected	12,850, 2448	4269, 1927	12,493, 2408	9271, 3303
Total, independent, R_{int}	0.0641	0.0396	0.0409	0.0664
λ (Mo Kα) (Å)	0.71073	0.71073	0.71073	0.71073
R_1, $wR_2[I > 2\sigma(I)]$	0.0360, 0.0734	0.0333, 0.0829	0.0408, 0.0613	0.0496, 0.0951

Table 2
Selected bond lengths (Å) and bond angles (°) for **1**

Pr(1)–O(1)	2.416(3)	Pr(1)–O(3)#4	2.540(4)
Pr(1)–O(1)#3	2.416(3)	Pr(1)–O(3)#5	2.540(4)
Pr(1)–O(2)#1	2.367(4)	Pr(1)–O(5)	2.571(4)
Pr(1)–O(2)#2	2.367(4)	Pr(1)–O(5)#3	2.571(4)
O(1)–Pr(1)–O(1)#3	142.12(18)	O(2)#1–Pr(1)–O(3)#4	149.55(12)
O(1)–Pr(1)–O(2)#1	102.72(13)	O(2)#1–Pr(1)–O(3)#5	74.04(12)
O(1)–Pr(1)–O(2)#2	91.21(13)	O(2)#1–Pr(1)–O(5)	73.25(12)
O(1)–Pr(1)–O(3)#4	73.38(12)	O(2)#1–Pr(1)–O(5)#3	71.67(13)
O(1)–Pr(1)–O(3)#5	76.91(12)	O(2)#2–Pr(1)–O(3)#4	74.04(12)
O(1)–Pr(1)–O(5)	73.21(13)	O(2)#2–Pr(1)–O(3)#5	149.55(12)
O(1)–Pr(1)–O(5)#3	144.58(12)	O(2)#2–Pr(1)–O(5)	71.67(13)
O(1)#3–Pr(1)–O(2)#1	91.21(13)	O(2)#2–Pr(1)–O(5)#3	73.25(12)
O(1)#3–Pr(1)–O(2)#2	102.72(13)	O(3)#4–Pr(1)–O(3)#5	75.70(16)
O(1)#3–Pr(1)–O(3)#4	76.91(12)	O(3)#4–Pr(1)–O(5)	130.82(13)
O(1)#3–Pr(1)–O(3)#5	73.38(12)	O(3)#4–Pr(1)–O(5)#3	128.77(12)
O(1)#3–Pr(1)–O(5)	144.58(12)	O(3)#5–Pr(1)–O(5)#3	130.82(13)
O(1)#3–Pr(1)–O(5)#3	73.21(13)	O(3)#5–Pr(1)–O(5)	128.77(12)
O(2)#1–Pr(1)–O(2)#2	136.34(19)	O(5)–Pr(1)–O(5)#3	71.73(17)

Symmetry operation: #1, $-x+1$; $-y+1$; $-z$. #2, x; $-y+1$; $z-1/2$. #3, $-x+1$; y; $-z-1/2$. #4 $-x+1/2$; $-y+1/2$; $z-1/2$. #5, $x+1/2$; $-y+1/2$; $-z$.

(15 mg) yield. Anal. Calcd for $C_{21}ErH_{16}O_8$: C, 44.71; H, 2.86. Found: C, 44.42; H, 2.49. IR data (KBr pallet, $\nu\,cm^{-1}$): 569 (w), 678 (m), 772 (s), 854 (s), 1004 (w), 1181 (w), 1418 (s), 1517 (s), 1579 (s), 1606 (m), 3392 (s).

3. Results and discussion

3.1. Structure description

Crystal data for **1–4** are shown in Table 1 and the selected bond lengths and angles of **1–4** are listed in Tables 2–5. The crystallographic data of **1–3** show that they are isostructural and herein only complexes **2** and **4** will be described in detail. In **2**, Eu(1) is eight-coordinated by six oxygen atoms (O1, O1A, O2A, O2B, O4D, O4E) from six carboxylate groups of six 4,4′-Hbpdc ligands in monodentate and bridging modes, and two oxygen atoms (O5, O5A) of two water molecules (Fig. 1). The Eu–O (carboxyl) bond lengths range from 2.287(5) to 2.492(5) Å and the mean distance of that is 2.379 Å, while the Eu–O (water) bond lengths are both 2.512(5) Å, which are all similar to that in lanthanide 2,2′-biphenyldicarboxylate complexes [14,15].

There is only one coordination mode of 4,4′-Hbpdc ligand present in **2** (Scheme 1a). One carboxyl group of 4,4′-Hbpdc

Table 3
Selected bond lengths (Å) and bond angles (°) for **2**

Eu(1)–O(1)	2.357(5)	Eu(1)–O(4)#4	2.492(5)
Eu(1)–O(1)#3	2.357(5)	Eu(1)–O(4)#5	2.492(5)
Eu(1)–O(2)#1	2.287(5)	Eu(1)–O(5)	2.512(5)
Eu(1)–O(2)#2	2.287(5)	Eu(1)–O(5)#3	2.512(5)
O(1)–Eu(1)–O(1)#3	98.5(3)	O(2)#1–Eu(1)–O(4)#4	74.07(19)
O(1)–Eu(1)–O(2)#1	92.32(19)	O(2)#1–Eu(1)–O(4)#5	101.96(18)
O(1)–Eu(1)–O(2)#2	169.17(18)	O(2)#1–Eu(1)–O(5)	104.30(19)
O(1)–Eu(1)–O(4)#4	73.87(17)	O(2)#1–Eu(1)–O(5)#3	72.12(18)
O(1)–Eu(1)–O(4)#5	108.01(18)	O(2)#2–Eu(1)–O(4)#4	101.96(18)
O(1)–Eu(1)–O(5)	112.00(18)	O(2)#2–Eu(1)–O(4)#5	74.07(19)
O(1)–Eu(1)–O(5)#3	72.51(19)	O(2)#2–Eu(1)–O(5)	72.12(18)
O(1)#3–Eu(1)–O(2)#1	169.17(18)	O(2)#2–Eu(1)–O(5)#3	104.30(19)
O(1)#3–Eu(1)–O(2)#2	92.32(19)	O(4)#4–Eu(1)–O(4)#5	45.6(2)
O(1)#3–Eu(1)–O(4)#4	108.01(18)	O(4)#4–Eu(1)–O(5)	174.07(18)
O(1)#3–Eu(1)–O(4)#5	73.87(17)	O(4)#4–Eu(1)–O(5)#3	130.49(19)
O(1)#3–Eu(1)–O(5)	72.51(19)	O(4)#5–Eu(1)–O(5)	130.49(19)
O(1)#3–Eu(1)–O(5)#3	112.00(18)	O(4)#5–Eu(1)–O(5)#3	174.07(18)
O(2)#1–Eu(1)–O(2)#2	76.9(3)	O(5)–Eu(1)–O(5)#3	52.9(3)

Symmetry operation: #1, x; $-y+2$; $z-1/2$. #2, $-x+2$; $-y+2$; $z-1/2$. #3, $-x+2$; y; z. #4, $-x+3/2$; $-y+3/2$; $z-1/2$. #5, $x+1/2$; $-y+3/2$; $z-1/2$.

Table 4
Selected bond lengths (Å) and bond angles (°) for **3**

Gd(1)–O(1)	2.349(3)	Gd(1)–O(3)#4	2.472(3)
Gd(1)–O(1)#3	2.349(3)	Gd(1)–O(3)#5	2.472(3)
Gd(1)–O(2)#1	2.295(3)	Gd(1)–O(5)	2.509(3)
Gd(1)–O(2)#2	2.295(3)	Gd(1)–O(5)#3	2.509(3)
O(1)–Gd(1)–O(1)#3	142.76(16)	O(2)#1–Gd(1)–O(3)#4	149.58(11)
O(1)–Gd(1)–O(2)#1	100.96(11)	O(2)#1–Gd(1)–O(3)#5	73.71(11)
O(1)–Gd(1)–O(2)#2	92.61(11)	O(2)#1–Gd(1)–O(5)	72.95(11)
O(1)–Gd(1)–O(3)#4	74.23(11)	O(2)#1–Gd(1)–O(5)#3	72.20(11)
O(1)–Gd(1)–O(3)#5	76.62(11)	O(2)#2–Gd(1)–O(3)#4	73.71(11)
O(1)–Gd(1)–O(5)	72.89(11)	O(2)#2–Gd(1)–O(3)#5	149.58(11)
O(1)–Gd(1)–O(5)#3	144.29(11)	O(2)#2–Gd(1)–O(5)	72.20(11)
O(1)#3–Gd(1)–O(2)#1	92.61(11)	O(2)#2–Gd(1)–O(5)#3	72.95(11)
O(1)#3–Gd(1)–O(2)#2	100.96(11)	O(3)#4–Gd(1)–O(3)#5	75.98(15)
O(1)#3–Gd(1)–O(3)#4	76.62(11)	O(3)#4–Gd(1)–O(5)	130.70(10)
O(1)#3–Gd(1)–O(3)#5	74.23(11)	O(3)#4–Gd(1)–O(5)#3	128.76(10)
O(1)#3–Gd(1)–O(5)	144.29(11)	O(3)#5–Gd(1)–O(5)	128.76(10)
O(1)#3–Gd(1)–O(5)#3	72.89(11)	O(3)#5–Gd(1)–O(5)#3	130.70(10)
O(2)#1–Gd(1)–O(2)#2	136.67(17)	O(5)–Gd(1)–O(5)#3	71.63(15)

Symmetry operation: #1, $-x+1$; $-y+1$; $-z$. #2, x; $-y+1$; $z-1/2$. #3, $-x+1$; y; $-z-1/2$. #4, $-x+1/2$; $-y+1/2$; $z-1/2$. #5, $x+1/2$; $-y+1/2$; $-z$.

Table 5
Selected bond lengths (Å) and bond angles (°) for **4**

Er(1)–O(1)	2.283(6)	Er(1)–O(5)	2.399(6)
Er(1)–O(2)#1	2.277(6)	Er(1)–O(6)	2.371(7)
Er(1)–O(3)#2	2.368(7)	Er(1)–O(7)	2.345(6)
Er(1)–O(4)#2	2.452(6)	Er(1)–O(8)	2.363(7)
O(1)–Er(1)–O(2)#1	101.5(2)	O(3)#2–Er(1)–O(5)	102.1(3)
O(1)–Er(1)–O(3)#2	81.3(2)	O(3)#2–Er(1)–O(7)	78.0(2)
O(1)–Er(1)–O(4)#2	77.8(2)	O(3)#2–Er(1)–O(8)	131.1(2)
O(1)–Er(1)–O(5)	154.9(2)	O(4)#2–Er(1)–O(5)	84.1(2)
O(1)–Er(1)–O(6)	149.2(2)	O(4)#2–Er(1)–O(6)	113.2(3)
O(1)–Er(1)–O(7)	79.2(2)	O(4)#2–Er(1)–O(7)	129.6(2)
O(1)–Er(1)–O(8)	78.4(2)	O(4)#2–Er(1)–O(8)	77.8(2)
O(2)#1–Er(1)–O(3)#2	155.6(2)	O(5)–Er(1)–O(6)	54.9(2)
O(2)#1–Er(1)–O(4)#2	149.8(2)	O(5)–Er(1)–O(7)	125.9(2)
O(2)#1–Er(1)–O(5)	85.6(2)	O(5)–Er(1)–O(8)	81.0(2)
O(2)#1–Er(1)–O(6)	83.0(3)	O(6)–Er(1)–O(3)#2	82.8(3)
O(2)#1–Er(1)–O(7)	78.8(2)	O(6)–Er(1)–O(7)	71.8(2)
O(2)#1–Er(1)–O(8)	72.6(2)	O(6)–Er(1)–O(8)	131.1(2)
O(3)#2–Er(1)–O(4)#2	54.6(2)	O(7)–Er(1)–O(8)	138.9(3)

Symmetry operation: #1, $-x+1$; $-y$; $-z+1$. #2, $-x$; $y+1/2$; $-z+1/2$.

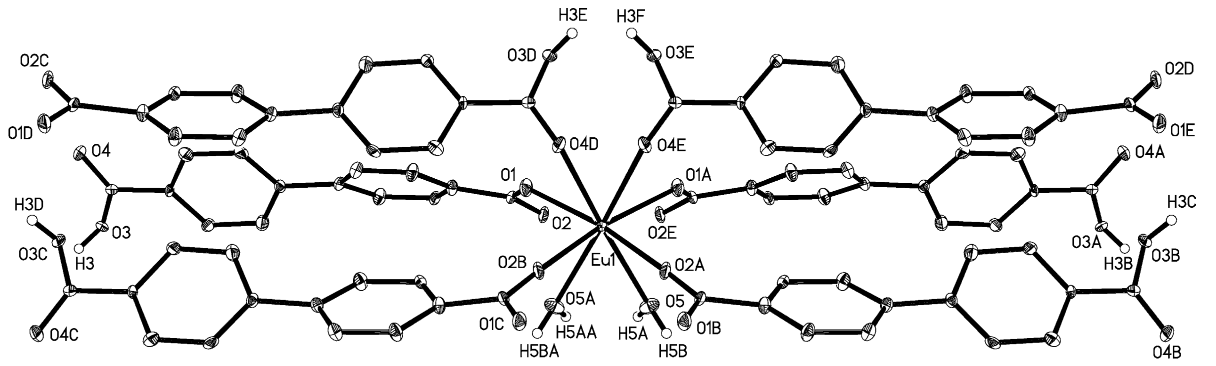

Fig. 1. The coordination environment of Eu(III) ion of **2** with thermal ellipsoids at 25% probability, and the occupancy of hydrogen atoms is 50%.

ligand is deprotonated, which bridges two Eu(III) ions in bridging bidentate fashion, whereas the other carboxyl group is undeprotonated and links one Eu(III) ion in monodentate mode. Therefore, each 4,4′-Hbpdc ligand acts as μ_3-bridge connecting three Eu(III) ions and each Eu(III) ion is coordinated to six 4,4′-bpdc ligands to form a 3D structure (Fig. 2). Two adjacent Eu(III) ions are bridged by carboxyl groups with nearest Eu···Eu distance of 5.041 Å.

In the 3D structure of **2**, the Eu(III) ions are arranged on the layers parallel to *bc* plane and the carboxyl groups of 4,4′-Hbpdc ligands link two adjacent Eu(III) ion layers along *a* axis to build up a sandwich 3D architecture with the distance between parallel Eu(III) ion layers of approximately 13.78 Å.

There is only one coordination environment of Er(III) ions in **4**: Er(1) is coordinated by four carboxyl oxygen atoms (O5, O6, O3B and O4B) from two carboxyl groups of two 4,4′-bpdc ligands in chelating bidentate coordination mode, two carboxyl oxygen atoms (O1 and O2A) from two carboxyl groups of two 4,4′-bpdc ligands in bridging mode, and two oxygen atoms (O7 and O8) of two water molecules (Fig. 3). The bond lengths of Er–O (carboxyl) are in the range of 2.277(6)–2.452(6) Å, and the mean distances of Er–O (carboxyl) and Er–O (water) are 2.358 and 2.354 Å, respectively.

The 4,4′-bpdc ligand adopts two types of coordination mode in **4**: (a) two carboxyl groups of a 4,4′-bpdc ligand are both deprotonated and one connects two Er(III) ions in bridging bidentate fashion, while the other connects one Er(III) ion in chelating bidentate mode (Scheme 1b); (b) each carboxyl group of a 4,4′-bpdc ligand is coordinated to one Er(III) ion in chelating bidentate mode (Scheme 1c). Thus, the 4,4′-bpdc ligands act as μ_3- and μ_2-bridges to link

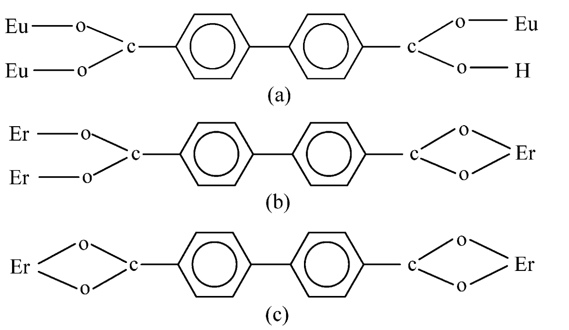

Scheme 1. Coordination modes of bpdc ligand in **2** (a) and **4** (b,c).

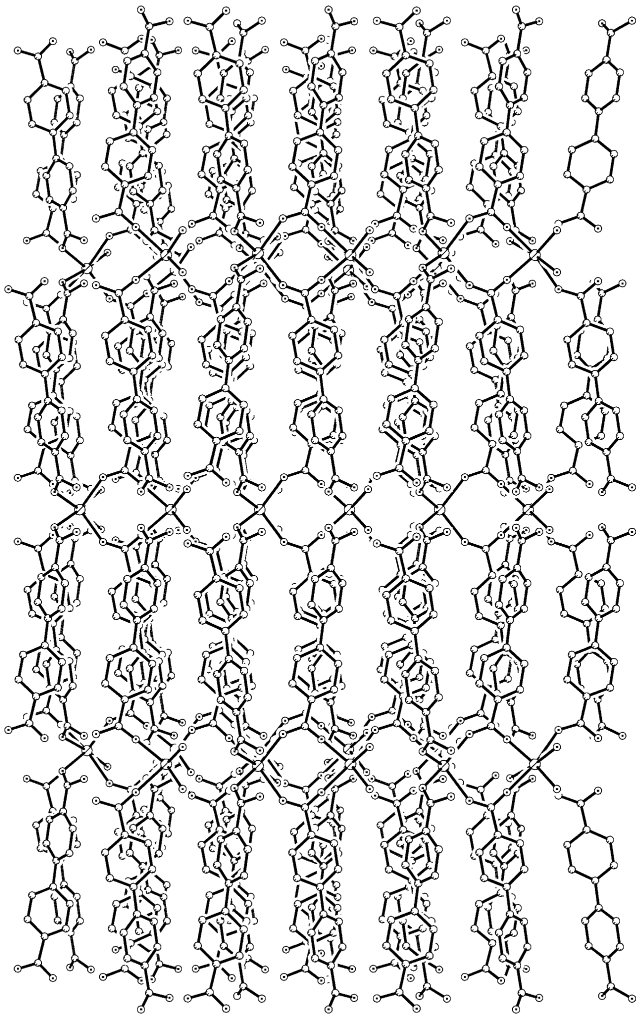

Fig. 2. The sandwich 3D structure of **2** viewed along *b* axis, all hydrogen atoms are omitted for clarity.

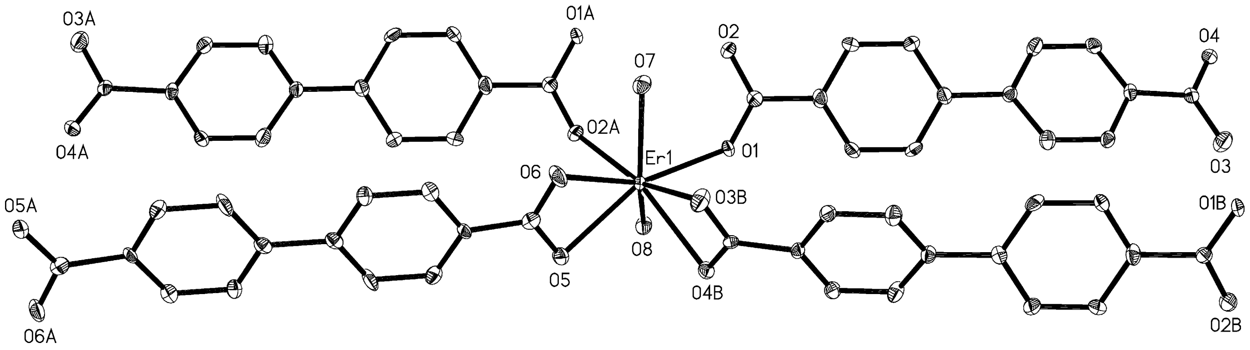

Fig. 3. The coordination environment of Er(III) ion of **4** with thermal ellipsoids at 25% probability. All hydrogen atoms are omitted for clarity.

three Er(III) ions and two Er(III) ions, respectively, and each Er(III) ion attaches to four 4,4′-bpdc ligands to construct a 3D structure.

In **4**, the Er(III) ions are located on the layers parallel to *bc* plane with the distance between the metal layers of approximately 14.4 Å and linked up by 4,4′-bpdc ligands to construct pillared sandwich 3D structure. Similar to **2**, two adjacent Er(III) ions are bridged by carboxyl groups of 4,4′-bpdc ligands displaying the nearest Er···Er distance of 4.784 Å.

Compared the crystal data of **2** with those of **4**, the Ln(III) ions interlayer distance of **2** (13.78 Å) is shorter than that of **4** (14.4 Å), although the ionic radius of Eu(III) ion is larger than that of Er(III) ion due to the lanthanide contraction effect. This maybe result from the steric effect of the 4,4′-Hbpdc ligands which are a little out of the perpendicularity in **2**, while they are relatively erect in **4**, and the different coordination modes of 4,4′-H_2bpdc ligands with lanthanide ions in **2** and **4**.

In view of the crystal data of **1**, **2** and **3**, the mean distances of Pr–O (carboxyl), Eu–O (carboxyl) and Gd–O (carboxyl) are 2.441, 2.379 and 2.372 Å, respectively; the Pr–O (w) Eu–O (w) and Gd–O (w) distances are 2.571, 2.512 and 2.509 Å, respectively. The nearest separations of Pr···Pr, Eu···Eu and Gd···Gd are 5.056, 5.041, and 5.035 Å, respectively, and the distances between the two neighboring lanthanide ions layers are 13.85, 13.78 and 13.77 Å in **1**, **2**, and **3**, respectively. So we can conclude that Ln–O, Ln···Ln and Ln(III) ions interlayer distances decrease with the contraction of the ionic radii from Pr(III) to Gd(III) ions. From the coordination modes of the 4,4′-bpdc ligands, since the larger ionic radii of Pr(III), Eu(III) and Gd(III) ions than the radius of Er(III) ion, there are six 4,4′-bpdc ligands around one Pr(III), Eu(III) or Gd(III) ion in monodentate and bridging coordination fashions, while only four 4,4′-bpdc ligands around one Er(III) ion in bridging and chelating bidentate coordination modes, to complete the high coordination number of lanthanide ions.

Owing to the different positions of carboxyl groups of 4,4′-bpdc ligands from that of 2,2′-bpdc ligands, the structures of the title complexes are completely different from that of lanthanide complexes with 2,2′-bpdc ligand [14]. Thus, the carboxyl group positions of polycarboxylic acid ligands and the directionality of metal–ligand bonds play an important role in the construction of coordination polymers, and the linear dicarboxylic acid ligands are liable to form sandwich architecture.

3.2. Photophysical properties of 2

Complex **2** emits intense red fluorescence when it is irradiated by UV light Fig. 4 shows its emission spectrum excited at a wavelength of 355 nm at 77 K (a) and 298 K (b), corresponding to $^5D_0 \rightarrow {}^7F_J$ ($J = 0$–4) transitions in the range of 13,900–17,300 cm^{-1}. The $^5D_0 \rightarrow {}^7F_2$ transition is the induced electric dipole transition, which is

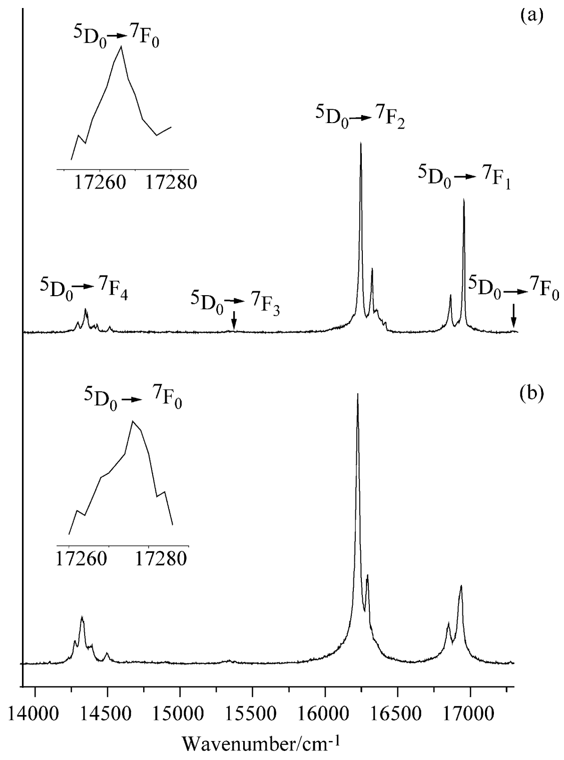

Fig. 4. Emission spectra of **2** corresponding to $^5D_0 \rightarrow {}^7F_J$ ($J = 0 \sim 4$) transitions at 77 K (a) and 298 K (b), $\lambda_{exc} = 355$ nm.

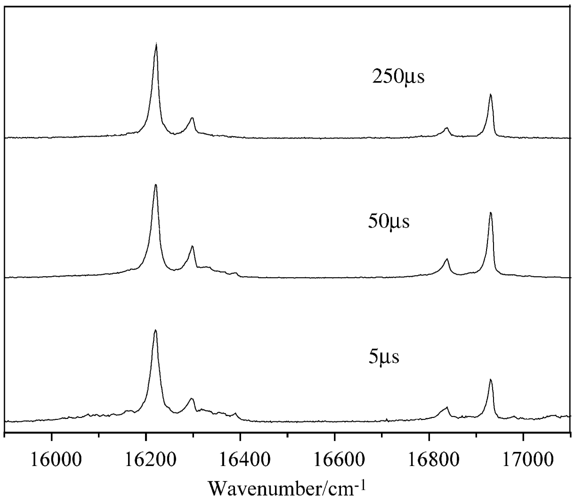

Fig. 5. The time-resolved spectra of **2** in the range of 17,100–15,900 cm^{-1} at 77 K, delay time: 5, 50 and 250 μs, $\lambda_{exc} = 355$ nm.

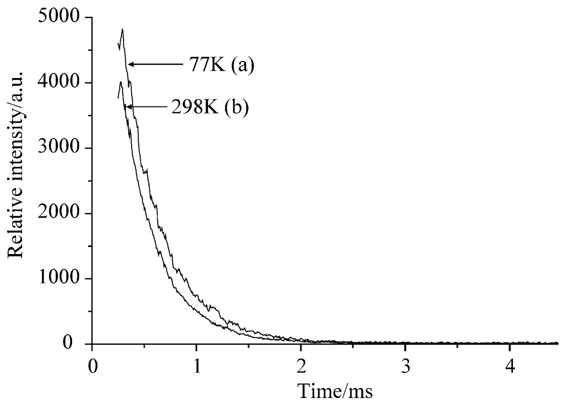

Fig. 6. The decay curves of **2** at 77 K (a) and 298 K (b), analyzing wave number: 16,223 cm^{-1} for 77 K, 16,237 cm^{-1} for 298 K.

hypersensitive and is greatly affected by the coordination environment, while the $^5D_0 \rightarrow {}^7F_1$ transition is the magnetic dipole transition, which is much less sensitive to the environment. The intensity ratio of $^5D_0 \rightarrow {}^7F_2/{}^5D_0 \rightarrow {}^7F_1$ is 2.1, which shows that the Eu^{3+} ions are not at an inversion center [17]. It is in good agreement with the results of single-crystal X-ray diffraction. Comparing the emission spectra of **2** at 77 k with that at 298 K, the low temperature emission spectrum of **2** shows the expected bathochromic shift and line-narrowing.

The time-resolved spectra of the complex **2** in the range of 17,100–15,900 cm^{-1} (corresponding to $^5D_0 \rightarrow {}^7F_1$ and $^5D_0 \rightarrow {}^7F_2$) at 77 K were recorded and are shown in Fig. 5. From Fig. 5, it can be seen that no significant change in the relative intensities, positions and shapes of the emission peaks takes place as the delay time varies, displaying a single Eu(III) ion site in **2**.

The decay curves of **2** (Fig. 6) show that the luminescence lifetimes of **2** are 0.355 ms at 298 K and 0.392 ms at 77 K, which shows that the lower-temperature lifetime is longer than the higher one due to the thermal deactivation at higher temperature.

4. Conclusions

Four new lanthanide coordination polymers, Ln(4,4′-Hbpdc)(4,4′-bpdc)$(H_2O)_2$ (Ln = Pr(**1**), Eu(**2**), Gd(**3**)) and Er(4,4′-bpdc)$_{1.5}(H_2O)_2$ (**4**), were synthesized by the solvothermal reaction and characterized by single crystal X-ray diffraction. The results of the X-ray structure analysis show that complexes **1–3** are isostructural and exhibit 3D sandwich structure formed by lanthanide ion layers and 4,4′-bpdc ligand layers alternately linking up with each other. Complex **4** also possess 3D sandwich structure similar to **1**–**3**. The crystal structures of the title complexes are quite different from the structures of lanthanide complexes with 2,2′-bpdc ligand owing to the positions of carboxyl groups of bpdc ligands. Therefore, we conclude that the carboxyl group positions of polycarboxylic acid ligands and the directionality of metal–ligand bonds play an important role in the construction of coordination polymers, and the linear dicarboxylic acid ligands are liable to form sandwich architecture.

5. Supplementary

CCDC Nos 228764-228767 contains the supplementary crystallographic data for this paper. These data can be obtained free of charge at www.ccdc.cam.ac.uk/conts/retrieving.html [or from the Cambridge Crystallographic Data Centre, 12, Union Road, Cambridge CB2 1EZ, UK; fax: (internat.) +44-1223/336-033; E-mail: deposit@ccdc.cam.ac.uk].

Acknowledgements

This work is supported by National Natural Science Foundation of China (20331010).

References

[1] O.M. Yaghi, H. Li, C. Davis, D. Richardson, T.L. groy, Acc. Chem. Res. 31 (1998) 474.
[2] M.D. Hollingsworth, Science 295 (2002) 2410.
[3] O.M. Yaghi, M. O'Keefee, N. W. Ockwig, H. K. Chae, M. Eddaoudi, J. Kim, Nature 423 (2003) 705.
[4] N.L. Rosi, M. Eddaoudi, J. Kim, M. O'Keefee, O.M. Yaghi, Angew. Chem. Int. Ed. 41 (2002) 284.
[5] M.J. Zaworotko, Chem. Commun. (2001) 1.
[6] P. Day, J. Chem. Soc. Dalton Trans. (2000) 3483.
[7] C. Janiak, J. Chem. Soc. Dalton Trans. (2000) 3885.
[8] L. Pan, B.S. Finkel, X. Huang, J. Li, Chem. Commun. (2001) 105.
[9] G. Liu, B. Ye, Y. Ling, X. Chen, Chem. Commun. (2002) 1442.

[10] Y. Liang, M. Hong, R. Cao, J. Weng, W. Su, Inorg. Chem. Commun. 4 (2001) 599.
[11] L. Long, Y. Ren, L. Ma, Y. Jiang, R. Huang, L. Zheng, Inorg. Chem. Commun. 6 (2003) 690.
[12] L. Pan, N. Ching, X. Huang, J. Li, Inorg. Chem. 39 (2000) 5333.
[13] K. Seki, W. Mori, J. Phys. Chem. B 106 (2002) 1380.
[14] Y. Wang, X. Zheng, W. Zhang, L. Jin, Eur. J. Inorg. Chem. 7 (2003) 1355.
[15] Y. Wang, X. Zheng, W. Zhuang, L. Jin, Eur. J. Inorg. Chem. 19 (2003) 3572.
[16] G.M. Sheldrick, SHELX-97, PC-Version, University of Göttingen, Germany, 1997.
[17] J.-C.G. Bünzli, in: J.-C. G. Bünzli, G. R. Choppin (Eds.), Lanthanide Probes in Life, Chemical and Earth Sciences: Theory and Practice, Elsevier, Amsterdam, 1989, (Chapter 7).